# High-density WGM Probes Generated by a ChG Ring Resonator for High-density 3D Imaging and Applications

P. Youplao[1, 2], N. Pornsuwancharoen[3], S. Suwanarat[4], K. Chaiwong[5], M.A. Jalil[6], I.S. Amiri[7], J. Ali[8], G. Singh[9], P. Yupapin [1, 2*], and K.T.V. Grattan[10]

[1]Computational Optics Research Group, Advanced Institute of Materials Science, Ton Duc Thang University, District 7, Ho Chi Minh City, 700,000, Vietnam;
[2]Faculty of Electrical & Electronics Engineering; Ton Duc Thang University, District 7, Ho Chi Minh City, 700,000, Vietnam;
[3]Department of Electrical Engineering, Faculty of Industry and Technology, Rajamangala University of Technology Isan, Sakon Nakhon Campus, Sakon Nakhon, 47160, Thailand;
[4]Department of Physics, Faculty of Science, Ramkhamheang University, Bangkok 1220, Thailand;
[5]Faculty of Industrial Technology, Leoi Rajabhat University, Leoi 42000, Thailand;
[6]Department of Physics, Faculty of Science, Universiti Teknologi Malaysia, 81310 Johor Bahru Malaysia, 81300 Johor Bahru, Malaysia;
[7]Division of Materials Science and Engineering, Boston University, Boston, MA, 02215, USA;
[8]Laser Center, IbnuSina Institute for Industrial and Scientific Research, UniversitiTeknologi Malaysia (UTM)
[9]Department of Electronics and Communication Engineering, Malaviya National Institute of Technology Jaipur, 302017, India;
[10]Department of Electrical & Electronic Engineering, School of Mathematics, Computer Science & Engineering, City, University of London, EC1V 0HB, United Kingdom;
*Corresponding author E-mail:preecha.yupapin@tdtu.edu.vn

**Abstract:** In this paper, the ultra-wideband source for light fidelity(LiFi) and high-density 3D imaging applications is proposed. The system consists of an add-drop multiplexer. The center ring is formed by the Chalcogenide glass (ChG), which is coupled with two GaAsInP/P side rings. The nonlinear effect within the side rings (phase modulators) is induced in the central ring. The superposition of light signals from side rings generates wider wavelength band, which makes the original input. The output is the set of squeezed light pulses known as whispering gallery mode(WGM)which is generated at the center of the system. Three different input sources are investigated, where the simulated results are comparatively plotted and discussed. The results show that the wavelength of 1.30 μm is the best input source. The output wavelengths band is ranged from 0.7-3.1 μm, which is suitable for LiFi source and high-density 3D imaging applications.

**Keywords:** High density light probe, Ultra-wideband source; LiFi source; ChG; Chalcogenide ring resonator;

## 1. Introduction

Chalcogenide glass(ChG) material has shown very interesting aspect that the propagation of light within a certain chalcogenide length changes due to the change in the refractive index [1, 2]. Several investigations have confirmed this observation [3-8]. Chalcogenide glass already exists and available for the potential applications [9-15]. One of the interesting aspects of light traveling within the ChG is that the change in wavelength range from the infrared to the radio wave (or microwave) that can be used to serve the current bandwidth requirements, where the light fidelity(LiFi) and wireless fidelity(WiFi) are required to use for the increasing bandwidths [16-19], where the individual system has been well established and available in the existing networks. However, the interconnection between LiFi and LiFi is expensive, therefore, the search for the new technology is ongoing. Up to date, the most of the employed chalcogenide lengths for the extended wavelength bands from 1.5-3.5 μm is within the range of few centimetres, where the results are reported of the applied chalcogenide lengths with the supercontinuum spectrum [20-22]. This means that the output wavelength can be used to supply in both lightwave and microwave source applications. However, the search for the new form of the device with more potential applications is continued. In this paper, we propose microring resonator that can be fabricated in micrometer dimensions with current fabrication facilities. Moreover, the external multiplexed/demultiplexed signals are also available by applying into the device ports. It is an add-drop filter, which is a micrometer scale. In simulations, we have investigated three different sources with the wavelengths of 1.10, 1.30, 1.55 microns. We have compared the results and selected one for further investigation. The desired targets are ultra-wideband wavelengths that can support wide ranges and the reasonable output power. Moreover, the ease of the connection is also the requirement, where the output at the center in the form of "WGM" can be suitable. Practically, the WGM output can be obtained by controlling the two side ring phase modulators [23-25]. The theoretical background is also reviewed. The simulation results are obtained by the Optiwave and MATLAB programs. Optiwave is used for preliminary investigations while MATLAB is utilized for detailed simulations.

## 2. Theoretical Review

In Figure1, a selected light source is input into the system via an input port, which is the input field ($E_{in}$ ) is the electrical field input. The electric fields are circulated within the system and described by the equations (1)-(9) [26], the input electric field is input into the z-axis, where $\boldsymbol{E_{in} = E_Z = E_0 e^{-ik_z t-\omega t}}$, $E_0$ is the initial electric field amplitude, Where $E_0$ is the electric field amplitude (real), $\boldsymbol{k_z}$ is the wave number in the direction of propagation (z-axis) and $\boldsymbol{\omega}$ is the angular frequency.

$$E_1 = \sqrt{1-\gamma_1}\,(\sqrt{1-\kappa_1}\,E_4 e^{-\frac{\alpha L_D}{2\,2}-jk_n\frac{L_D}{2}} + j\sqrt{\kappa_1}\;E_{in}\,e^{-\frac{\alpha L_D}{2\,4}-jk_n\frac{L_D}{4}}) \quad (1)$$

$$E_{R2} = E_{R1}\,e^{-\frac{\alpha}{2}L_R - jk_n L_R} \quad (2)$$

$$E_2 = \sqrt{1-\gamma_2}\,(\sqrt{1-\kappa_2}\,E_1 + j\sqrt{\kappa_2}\;E_{R2}) \quad (3)$$

$$E_3 = \sqrt{1-\gamma_3}\,(\sqrt{1-\kappa_3}\,E_2 e^{-\frac{\alpha L_D}{2\,2}-jk_n\frac{L_D}{2}} + j\sqrt{\kappa_3}\;E_{add}\,e^{-\frac{\alpha L_D}{2\,4}-jk_n\frac{L_D}{4}}) \quad (4)$$

$$E_{L2} = E_{L1}\,e^{-\frac{\alpha}{2}L_L - jk_n L_L} \quad (5)$$

$$E_4 = \sqrt{1-\gamma_4}\,(\sqrt{1-\kappa_4}\,E_3 + j\sqrt{\kappa_4}\;E_{L2}) \quad (6)$$

$$E_{dr} = \sqrt{1-\gamma_3}\,(\sqrt{1-\kappa_3}\,E_{add} + j\sqrt{\kappa_3}\,E_2\,e^{-\frac{\alpha L_D}{2\,4}-jk_n\frac{L_D}{4}}) \quad (7)$$

$$E_{th} = \sqrt{1-\gamma_1}\,(\sqrt{1-\kappa_1}\,E_{in} + j\sqrt{\kappa_1}\,E_4\,e^{-\frac{\alpha L_D}{2\,4}-jk_n\frac{L_D}{4}}) \quad (8)$$

$$E_{out} = \sqrt{1-\gamma_3}\,(\sqrt{1-\kappa_3}\,E_{dr}^{*} + j\sqrt{\kappa_3}\,E_2\,e^{-\frac{\alpha L_D}{2\,4}-jk_n\frac{L_D}{4}}) \quad (9)$$

Where $E_{dr}^{*} = -nE_{dr}$ , where the complex conjugate electrical field is the phase term is involved and presented the microring circuit $\kappa$ is the coupling factor, $\gamma$ is the intensity insertion loss coefficient of the directional coupler, $\alpha$ is the intensity attenuation coefficient of the ring, where $kn = 2\pi \cdot n_{eff}$, $n_{eff}$ = the effective refractive index. n is the reflection ratio. $L_D$= the circumference of the center ring, $L_R$ is the circumference of the right ring, $L_L$ is the circumference of the left ring. If there is without the reflected signal for the ended ports, the reflected electric filed power has vanished.

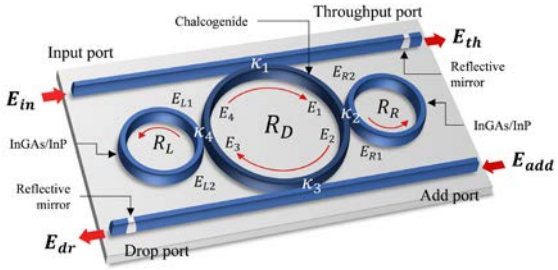


**Figure 1:** A schematic of the microring conjugate mirror, where $\boldsymbol{E_{in}}$, $\boldsymbol{E_{th}}$, $\boldsymbol{E_{dr}}$, and $\boldsymbol{E_{add}}$ are the optical field of the input, throughput, drop, and add port, respectively. $R_L$: Left-hand ring radius, $R_R$: Right-hand ring radius, $R_D$: Center ring radius, $\boldsymbol{\kappa_s}$: coupling constants, which is 0.5 for all $\boldsymbol{\kappa_s}$. The center ring is the ChG material. In this case the the reflected coefficient is neglected.

## 3. Simulation Results

It is established that the wavelength of the light propagates in the chalcogenide glass due to the change in refractive index of the propagated materials. However, most of the published works have reported the requirement of a few tens of centimeters of chalcogenide length [3-5]. In contrast, we have found that the length of the chalcogenide glass can be shortened by inducing the nonlinear effect couple into the propagation medium. Hence, we have proposed a device with an on-chip design called as a modified add-drop filter It consists of a center ring is formed by a length of a chalcogenide glass about few µm surrounded by two nonlinear phase modulators [27]. They are made of GaAsInP/P material in smaller ring radius. The nonlinear effect of light travelling within the side rings is induced into the chalcogenide ring and increase its refractive index. By using the obtained preliminary results, the required outputs and parameters are obtained. The simulation results are obtained by using the MATLAB program, in which the comparative wavelength input sources are 1.10, 1.30 and 1.55 µm. The graphical result is shown in Figure 2. Other characteristics of light propagating within the on-chip system in Figure 1 are plotted in Figures 2-6. Linear and nonlinear refractive indices of the GaAsInP/P are 3.14 and $1.30\text{x}10^{-13}$ $m^2W^{-1}$[27], respectively. The attenuation coefficient of the waveguide is 0.1 dB $(mm)^{-1}$, $A_{eff}$ = 0.50 $\mu m^2$. For simplicity, the waveguide loss is 0.5 for all wavelengths. The ChG dimension is given in the figure captions, $A_{eff}$ = 0.39 $\mu m^2$, the nonlinear refractive index $n_2 = 8.6 \times 10^{-18}$ $m^2/W$ [21], linear refractive index $n_0$ = 2.63 [28]. The loss parameter $\alpha$ = 3.2 dB$cm^{-1}$ [27], the fractional intensity loss $\gamma$ = 0.1 and other used parameters are given in the related figure captions. There were 3 different input sources used in the simulation.

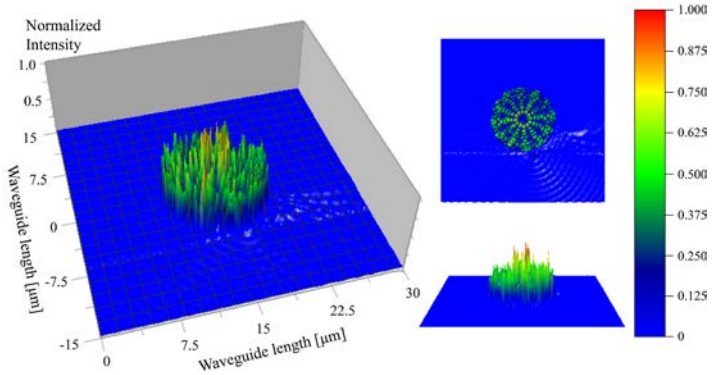


**Figure 2**: The Optiwave results of the system, where the (InGAs/InP) $R_l$=2.22 µm, ChG $R_l$=6 µm, (***InGAs/InP***) $R_r$=2.19 µm, the input center wavelength is 1.10 µm, the other parameters are given in the result description section. The high-density outputs in terms of wavelength is seen.

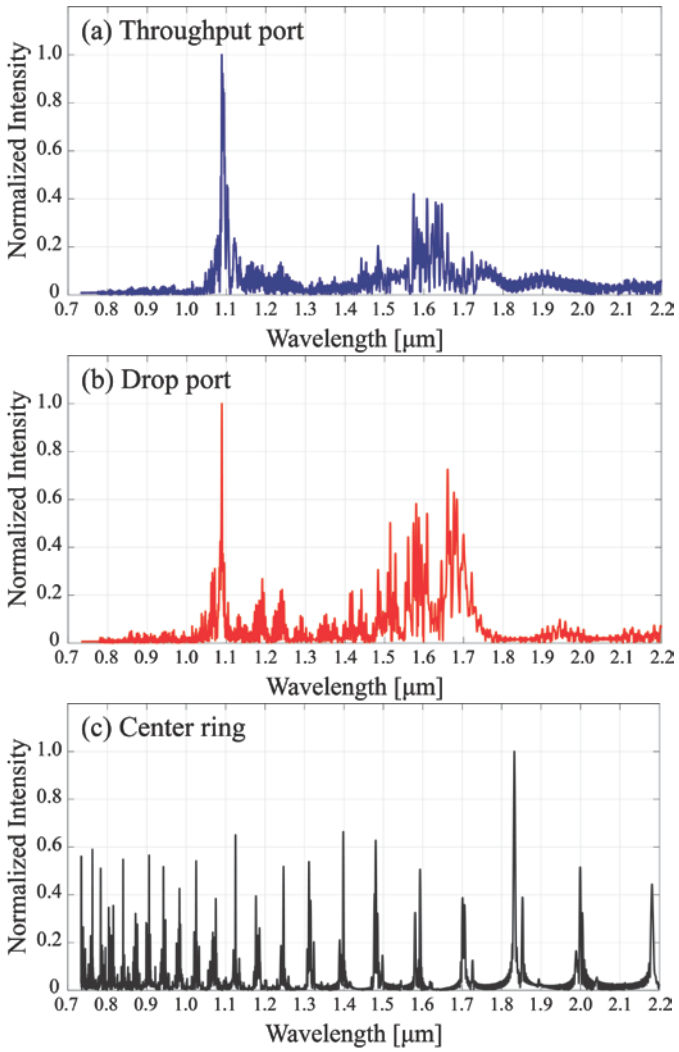


**Figure 3**: The results of the ultra-wideband wavelengths, the input light power of 10 mW with the center wavelength is at 1.10 µm. The ring system's parameters are the same in Fig 2. The output wideband wavelength from 0.7-2.2 µn is obtained. The wideband wavelength outputs are also seen at the throughput and drop ports.

The MATLAB program was used in the simulation. The output of the device is shown in Figure 3, where (a) and (b) are throughput and drop port signals, (c) is the WGM output. The plot of the relationship between the input power and WGM output of the wavelength sources is plotted in Fig. 4, which shows that the maximum power of the light source is at the wavelength of 1.30 micron. The ultra-wideband outputs of the employed sources are plotted in Figure 3, which is shown that the output at the center system can be wider extended than the original input sources. The obtained

wavelengths are ranged from 0.70-3.0 µm, which can be used for the transmission of both fiber optic and wireless signals by a single source. By using the two phase modulators, the extended wavelength bands and the amplified signals can be obtained within a tiny device. The results of the WGM outputs of the 3 wavelengths, 1.10, 1.30, 1.55 µm are shown in Figure 5, where the input power is at 2 mW, the ultra-wideband wavelengths are ranged from 0.70-3.1 µm. The output of the dense WGM probes at the add port is input into the image display device, which is the same system as shown in Figure 2. By using the same parameters. the in this case, the device is operated as the microring conjugate mirror(MCM). In Figure 6, the used reflection coefficient is 0.10(10%) at the input light source center wavelntg center is 1.10. The high-density 3D imaging display is obtained, which can be used for the high-density 3D imaging and printing applications. Moreover, such a device is formed at an on-chip scale that can be fabricated with the existing fabrication technology.

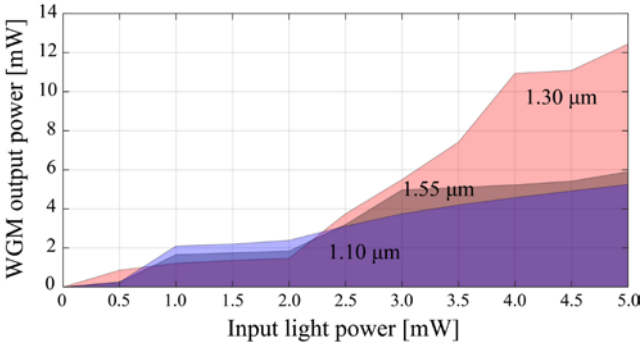


**Figure 4: The** plot the WGM outputs at the center of the system with the input power variation. The comparison of the 3 input wavelength sources, the changes in the input power are from 0.5-5.0 mW. The highest output is seen at the center wavelngth of 1.30 µm.

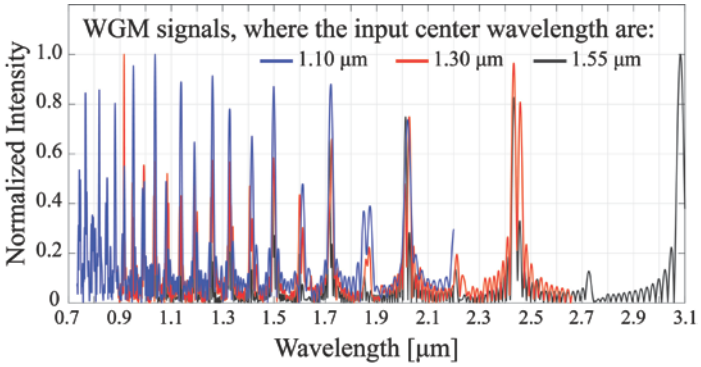


**Figure 5:** The MATLAB results of the WGM outputs of the 3 wavelengths. The input power is fixed at 2 mW, the input source center wavelengths are at 1.10 µm (blue), 1.30 µm (red), and 1.55 µm (black), the output wavengths are ranged from 0.7-3.1 µm.

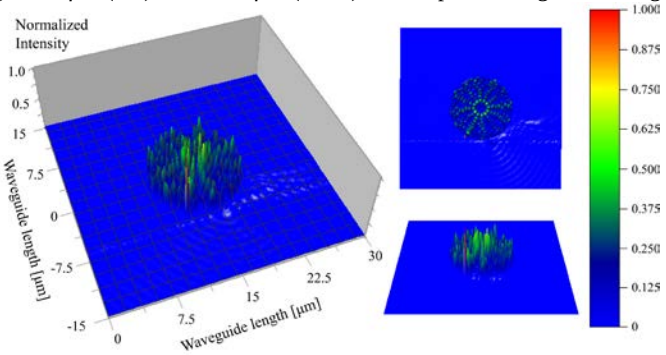


**Figure 6:** The Optiwave output of the dense WGM imaging output from the wavelength cenetr at 1.10 µm, in which the used parameters are the same. The add port output from the system in Figure 1(microring conjugate mirror) is input into the input of the 2nd system(the same as the 1st system), the reflection coefficient is 0.10(10%). The dense imaging display of the 3D image is obtained, which can be used for 3D dense imaging and printing applications.

## 4. Conclusion

We have proposed an on-chip scale system with potential application for ultra-wideband LiFi source, where currently each technique has the individual source. By using the proposed system, the wideband source can be merged into a single system. This means that the system redundancy can be reduced and a compact system can be featured. The newly

synthesized material is known as the chalcogenide glass can be used to form the wavelength conversion in the form of an add-drop filter, in which the output can be generated in the form of the WGM of light at the center of the system, which is convenient for LiFi application. The center ring signals are generated by the nonlinear effect induced by the side phase modulator, which is made of the GaAsInP/P. From the results obtained it is found that the output of the light source with the wavelength of 1.30 micron is a suitable input source for the system, where the use on the proposed device for LiFi sources and high-density 3D imaging applications is plausible. The ultra-wideband 0.70-3.1 μm can be achieved with a maximum output of 12 mW.

## Acknowledgments

The authors would like to give the appreciation for the research financial support by GUP project (Tier2 15J57) and Flagship UTM Shine Project (03G82) to the Universiti Teknologi Malaysia, Johor Bahru, Malaysia.

## References

[1] B.J. Eggleton, B.L. Davies, K. Richardson, Chalcogenide photonics, Nature Photonics, 5, pp. 141-148(2011).

[2] H. Lin, Y. Song, Y. Huang, D. Kita, S.D. Jones, K. Wang, L. Li, J. Li, H. Zheng, Z. Luo, H. Wang, S. Novak, A. Yadav, C.C. Huang, R.J. Shiue, D. Englund, T. Gu, D. Hewak, K. Richardson, J. Kong and J. Hu, Chalcogenide glass-on-graphene photonics, Nature Photonics, 11, 798–805 (2017).

[3] S. Vyas, T. Tanabe, M. Tiwari, and G. Singh," A Chalcogenide Photonic Crystal Fiber for Ultraflat Mid-infrared Supercontinuum Generation", Chi. Opt. Lett.14 (12), 123201-1 -123201-5(2016).

[4] A. Agrawal, M. Tiwari, Y.O. Azabi, V. Janyani, B.M.A. Rahman and K.T.V. Grattan," Ultrabroad supercontinuum generation in tellurite equiangular spiral photonic crystal fiber", J. of Mod. Opt. 60 (12), 956-962(2013).

[5] M.R. Karim, B.M.A. Rahman, and G.P. Agrawal, "Mid-infrared supercontinuum generation using dispersion-engineered Ge11:5As24Se64:5 chalcogenide channel waveguide", Opt. Exp. 23(5), 6903-69014 (2015).

[6] V. Shiryaev, and M. Churbanov, "Trends and prospects for development of chalcogenide fibers for mid-infrared transmission", J. Non-Cry. Sol.377 225–230 (2013).

[7] P. Ma, D.Y. Choi, Y. Yu, X. Gai, Z. Yang, S. Debbarma, S. Madden, and B. Luther-Davies, " Low-loss chalcogenide waveguides for chemical sensing in the mid-infrared", Opt. Exp. 21, 29927–29937(2013).

[8] M. El-Amraoui, G. Gadret,J. C. Jules, J. Fatome, C. Fortier, F. Désévédavy, I. Skripatchev, Y. Messaddeq,J. Troles, L. Brilland,W. Gao, T. Suzuki,Y. Ohishi, and F. Smektala," Microstructured chalcogenide optical fibers from As2S3 glass: towards new IR broadband sources", Opt. Exp.18(25),26655-26665(2010).

[9] J. Hu, C. R. Menyuk, L. B. Shaw, J. S. Sanghera, and I. D. Aggarwal, "Maximizing the bandwidth of supercontinuum generation in As2Se3 chalcogenide fibers," Opt. Exp., vol. 18, pp. 6722–6739(2010).

[10] I. D. Aggarwal and J. S. Sanghera, "Development and applications of chalcogenide glass optical fibers at NRL," J. Opt. Adv. Mater., vol. 4, pp. 665–678(2002).

[11] H. G. Dantanarayana, N. Abdel-Moneim, Z. Tang, L. Sojka, S. Sujecki, D. Furniss, A. B. Seddon, I. Kubat, O, Bang, and T, M. Benson, "Refractive index dispersion of chalcogenide glasses for ultra-high numerical-aperture fiber for mid-infrared supercontinuum generation" Opt. Mat. Exp., vol. 4, pp. 1444- 1455(2014).

[12] M.R. Karim, B.M.A. Rahman, G.P. Agrawal, "Mid-infrared supercontinuum generation using dispersion engineered Ge11.5As24Se64.5 chalcogenide channel waveguide", Opt. Exp., vol. 23, pp. 6903–6914(2015).

[13] P. Ma, D. Y. Choi, Y. Yu, X. Gai, Z. Yang, S. Debbarma, S. Madden, and B. Luther-Davies, "Low-loss chalcogenide waveguides for chemical sensing in the mid-infrared," Opt. Exp., vol. 21, pp. 29927–29937(2013).

[14] M. R. E. Lamont, B. Luther-Davies, D. Y. Choi, S. Madden, and B. J. Eggleton, "Supercontinuum generation in dispersion engineered highly nonlinear (g = 10 /W/m) As2S3 chalcogenide planar waveguide," Opt. Exp., vol. 16, pp. 14938–14944(2008).

[15] K. Ogusu, Y. Oda, "Modeling of the dynamic transmission properties of chalcogenide ring resonators in presence of fast and slow nonlinearities," Opt. Exp., vol. 19, pp. 649–659(2011).

[16] Basnayaka, A.D., and Hass, H., Aggregate signal interference of downlink LiFi networks, GLOBECOM 2017-2017 IEEE Global Communications Conference, 1-6(2017).

[17] Wu, X. and Pass, H., Access point assignment in hybrid LiFi and WiFi networks in consideration of LiFi channel blockage, 2017 IEEE 18th International Workshop on Signal Processing Advances in Wireless Communications(SPAWC), 1-5(2017).

[18] Wang, Y., Basayaka, D.A., Wu, X. and Pass, H., Optimization of Load Balancing in Hybrid LiFi/RF networks, IEEE Transactions on Communications, 65(4), 1708-1702(2017).

[19] Wu, X., Safari, M. and Hass, H., Joint optimization of load balancing and handover for hybrid LiFi and WiFi networks, 2017 IEEE Wireless Communications and Networking Conference(WCNC), 1-5(2017).

[20] Y. Yu, X. Gai, T. Wang, P. Ma, R. Wang, Z. Yang, D. Choi, S. Madden, and B. Luther-Davies, "Mid-infrared supercontinuum generation in chalcogenides," Opt. Exp., vol. 3, pp. 1075–1086(2013).

[21] P. Ma et al., "Low-loss chalcogenide waveguides for chemical sensing in the mid-infrared," Opt. Exp., vol. 21, pp. 29927–29937(2013).

[22] Y. Yu et al., "A broadband, quasi-continuous, mid-infrared supercontinuum generated in a chalcogenide glass waveguide," Laser Photon. Rev., vol. 8, pp. 792–798(2014).

[23] S. Soysouvanh, M.A. Jalil I.S. Amiri, J. Ali, G. Singh, S. Mitatha, P. Yupapin, K.T.V. Grattan, and M. Yoshida, 2018, Ultra-fast Electro-optic switching control using a soliton pulse within a modified add-drop multiplexer, Microsystem Technologies, 1-7(2018).

[24] Pornsuwancharoen, N., Youplao, P., Aziz, M.S., Ali, J., Amiri, I.S., Punthawanunt, S., Yupapin, P. and Grattan, K.T.V., In-situ 3D micro-sensor model using embedded plasmonic island for biosensors, Microsystem and Technologies, 1-5(2018).

[25] Phatharacorn, P., Chiangga, S. and Yupapin, P. , Analytical and simulation results of a triple micro whispering gallery mode probe system for a 3D blood flow rate sensor, Appl. Opt., 55(33), 009504(2016).

[26] J. Ali, N. Pornsuwancharoen, P. Youplao, M.S. Aziz, I.S. Amiri, K. Chaiwong, S. Chiangga, G. Singh, and P. Yupapin, Coherent light squeezing states within a modified microring system, Results in Physics, 9, 211-214(2018).

[27] Phatharaworamet, T., Teeka, C., Jomtarak, R., Mitatha, S. and Yupapin, P.P., 2010. Random binary code generation using dark-bright soliton conversion control within a Panda Ring resonator, J Lightwave Technol., 28(19), 2804-2809(2010).

[28] M.R. Karim, B.M.A. Rahman, G.P. Agrawal, "Mid-infrared supercontinuum generation using dispersion engineered Ge11.5As24Se64.5 chalcogenide channel waveguide", Opt. Exp., vol. 23, pp. 6903–6914(2015).